Energy distribution and lifetime of magnetospherically reflecting whistlers in the plasmasphere

J. Bortnik, U. S. Inan, and T. F. Bell

Space, Telecommunications, and Radio Science Laboratory, Electrical Engineering Department, Stanford University, Palo Alto, California, USA

Received 6 February 2002; revised 13 February 2003; accepted 4 March 2003; published 21 May 2003.

[1] Using ray tracing and Landau damping calculations based on recent data on suprathermal particle fluxes from the HYDRA instrument aboard the POLAR satellite, we estimate the energy distribution and the lifetimes of 0.2–10 kHz whistler mode waves in the plasmasphere. The rays are injected at 1000 km altitude and latitudes of 25°, 35°, 45°, and 55° to represent whistler wave energy originating in lightning discharges occurring in middle to low-latitude thunderstorms. The lifetime is defined as the time at which the wave power is reduced by 10 dB. Results indicate that the lifetime of whistler waves at lower frequencies is dramatically larger than those at higher frequencies and that rays injected at lower latitudes generally persist longer than those injected at higher latitudes in agreement with previous studies. An important characteristic of magnetospherically reflected (MR) whistlers is the strong tendency for whistler wave components at each frequency to eventually migrate to and settle into a multiply reflecting pattern at a specific (determined only by the wave frequency) *L*-shell, at which the wave energy would persist indefinitely in the absence of Landau damping and other losses. Consideration of this behavior together with the typical power spectrum of a single, vertical, cloud-to-ground lightning stroke, allows the estimation of the relative MR whistler wave energy in the inner magnetosphere as a function of *L*-shell. Results indicate that MR whistler energy deposition is maximized at the location of the slot region, suggesting that such MR whistlers launched by lightning discharges may be responsible for the enhanced diffusion rates and may play a more significant role than previously assumed in the formation and maintenance of the slot region between the inner and outer radiation belts. *INDEX TERMS:* 6984 Radio Science: Waves in plasma; 2730 Magnetospheric Physics: Magnetosphere—inner; 2753 Magnetospheric Physics: Numerical modeling; 2716 Magnetospheric Physics: Energetic particles, precipitating; 0689 Electromagnetics: Wave propagation (4275); *KEYWORDS:* slot-region, wave-particle interaction, Landau damping, magnetospherically reflected whistlers, lightning, ray tracing

Citation: Bortnik, J., U. S. Inan, and T. F. Bell, Energy distribution and lifetime of magnetospherically reflecting whistlers in the plasmasphere, *J. Geophys. Res.*, *108*(A5), 1199, doi:10.1029/2002JA009316, 2003.

1. Introduction

[2] Lightning generated whistler waves can propagate in the magnetosphere in the nonducted mode and form magnetospherically reflected (MR) whistler trains as originally observed by *Smith and Angerami* [1968] using data from the OGO1 and OGO3 satellites. These MR whistler trains typically persist for several seconds and remain geomagnetically trapped in the inner magnetosphere [*Smith and Angerami*, 1968]. The fundamental ability of whistlers to be reflected within the magnetosphere was first explained by *Kimura* [1966], who derived the dispersion relation with the inclusion of ions, demonstrating that the wave normal angle of the whistler wave could rotate past an angle of 90° (with respect to the static geomagnetic field) roughly reversing the ray's direction of propagation. A typical MR whistler ray path is shown in Figure 1a for a 500 Hz component injected at 25° geomagnetic latitude. As the whistler propagates through the magnetosphere, it is Landau damped due to interactions with the suprathermal particle population with the local rate of damping being determined by the wave frequency, the local ambient magnetic field and plasma density, the wave normal angle, and the particle distribution function [*Brinca*, 1972].

[3] MR whistlers have been previously studied by numerous authors, for example *Edgar* [1972], who has documented occurrence statistics in both geomagnetically quiet and active times and used extensive ray tracing to explain the observed upper and lower cutoff frequencies of MR whistlers [*Edgar*, 1976]; *Sonwalker and Inan* [1989], who have shown how such signals may upon many reflections evolve into an incoherent noise-like band; and *Draganov et al.* [1992, 1993] and *Thorne and Horne* [1994], who have studied the hypothesized relationship between MR whistlers and plasmaspheric hiss arriving at positive and negative

0148-0227/03/2002JA009316$09.00

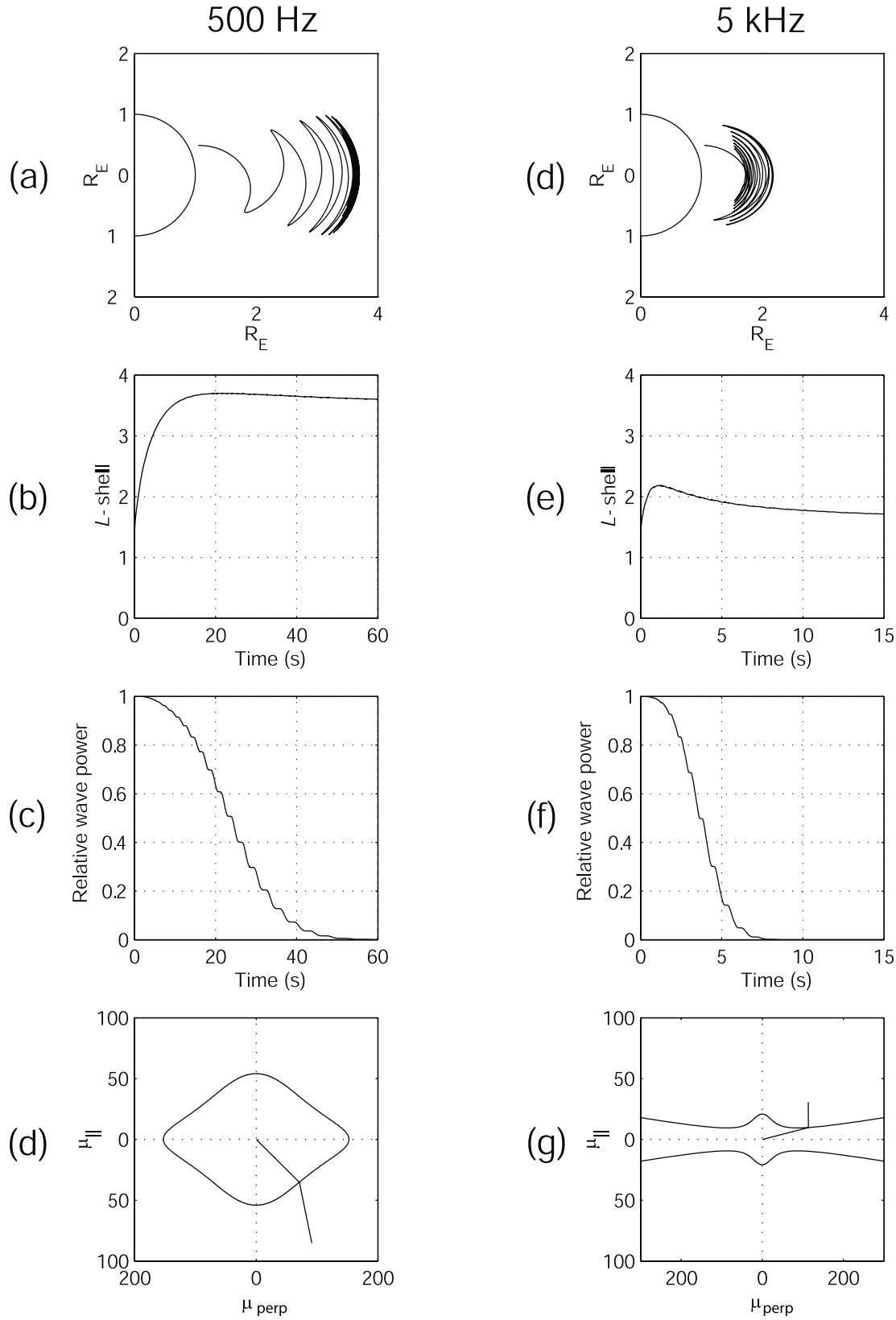

Figure 1. MR whistler ray path properties for two frequency components (left column: 0.5 kHz, right column 5 kHz) settling to a specific *L*-shell in the magnetosphere, (a) and (e) ray tracing plot, (b) and (f) Ray's local *L*-shell as a function of time, (c) and (g) power density damping of the ray due to parallel resonant interactions, (d) and (h) typical refractive index surfaces of the rays showing a closed refractive index surface, at the equator, on the second equatorial crossing (Figure 1d) and an open refractive index surface, at the equator, on the sixth equatorial crossing (Figure 1h).

conclusions respectively. More recent work has considered the quasi-resonant regime [*Lundin and Krafft*, 2001] and the interpretation of low-altitude satellite observations of transient flux enhancements in the drift loss cone as precipitation due to MR whistlers [*Blake et al.*, 2001; *Bortnik et al.*, 2002]. While the role of MR whistlers in the loss-rate of energetic radiation-belt electrons has been noted and estimated [*Abel and Thorne*, 1998a, 1998b], accurate models of the distribution of MR whistler wave power in the inner magnetosphere have not yet been available.

[4] In this work we provide a first-order estimate of the distribution of MR whistler wave energy as a function of *L*-shell. Our modeling starts with a broadband whistler wave injected into the magnetosphere at 1000 km altitude, with each wave frequency component propagating away from the Earth and tending to migrate to and settle on its "preferred" *L*-shell, thus undergoing spatial dispersion as discussed in section 2. The Landau damping of each frequency component along its propagation path is modeled using the Stanford VLF ray tracing code [*Inan and Bell*, 1977], in conjunction with the Landau damping formulation of *Brinca* [1972] and plasmaspheric suprathermal flux measurements from the HYDRA instrument aboard the POLAR satellite [*Bell et al.*, 2002]. In addition, we take into account the fact that each frequency component of the whistler carries a different power density at the injection latitude due to the particular frequency spectrum associated with the radiated fields of the lightning strike. Combining the lightning frequency spectrum and the frequency-dependent lifetime of MR whistlers allows us to quantify the MR whistler wave energy distribution in the inner magnetosphere.

2. Preferential Deposition of MR Wave Energy at Frequency-Specific *L*-Shells

[5] Lightning generated whistler waves injected into the magnetosphere typically contain a continuum of frequencies in the ELF and VLF bands. If the various frequency components of the whistler were to propagate in the magnetosphere indefinitely without being damped, each wave frequency component would tend to migrate within a few seconds to a "preferred" *L*-shell region, and subsequently slowly (tens of seconds) settle on a particular *L*-shell within that region in which the wave frequency is approximately equal to the equatorial lower hybrid resonance (LHR) frequency (discussed previously by *Thorne and Horne* [1994] and *Ristic'-Djurovic' et al.* [1998] and references therein). In this context the magnetosphere resembles a resonant cavity to whistler-mode waves, with the difference that at the reflection points it is the transverse component of the wave's magnetic field that vanishes, rather than the electric field.

[6] This ray path behavior is illustrated in Figure 1. The left column shows the ray path of a 500 Hz wave component injected at 25° geomagnetic latitude (Figure 1a), the *L*-shell of the ray as a function of time (Figure 1b), the relative wave power density as a function of time (Figure 1c), and a typical refractive index surface of the ray (Figure 1d). As shown in Figure 1b, the ray starts at $L \approx 1.4$ ($\lambda = 25°$ at 1000 km altitude), migrates to higher *L*-shells, and then slowly converges on its specific settling *L*-shell of $L \approx 3.45$. For comparison, Figure 1e shows a 5 kHz frequency component injected at the same latitude, $\lambda = 25°$, initially overshooting its specific settling *L*-shell and then slowly moving lower in altitude until it settles at $L \approx 1.6$. We note that for injection at midlatitudes, some frequency components move predominantly from lower to higher *L*-shells (e.g., Figures 1a and 1b), whereas others move predominantly from higher to lower *L*-shells (e.g., Figures 1e and 1f). Thus each *L*-shell is associated with a particular frequency component that is most likely to settle there, hereafter referred to as f_s. A plot of f_s (or alternatively the equatorial LHR frequency) as a function of *L*-shell is shown in Figure 3a. The degree to which wave energy is preferentially deposited at a particular *L*-shell is discussed in section 5 in connection with Figure 5.

3. Lifetime of MR Whistler Waves

[7] The damping due to parallel resonant interactions between whistler waves and suprathermal electrons (Landau damping) is computed using the formulation of *Brinca* [1972] and a distribution function of suprathermal electrons given by:

$$f(v) = 2 \times 10^5 / v^4 \ \left(\mathrm{cm}^{-6}\ \mathrm{s}^3\right) \qquad (1)$$

where v is the electron velocity measured in units of cm/s. This distribution represents an approximate numerical fit to measurements made with the HYDRA instrument on the POLAR satellite [*Bell et al.*, 2002] of electrons in the range 300 eV-2 keV, which are the energies of electrons most heavily involved in the Landau interaction. For reference, the corresponding flux values are $j(1\ \mathrm{keV}) = 10^5$ and $j(300\ \mathrm{eV}) = 3 \times 10^5\ \mathrm{cm}^{-2}\ \mathrm{s}^{-1}\ \mathrm{str}^{-1}\ \mathrm{keV}^{-1}$. It should be noted that the above flux values are substantially lower than those used by *Thorne and Horne* [1994] in their study. This discrepancy is discussed by *Bell et al.* [2002] and appears to be due to the fact that the model fluxes for $L < 4$ used by Thorne and Horne were based on spacecraft measurements made on a few passes in the outer plasmasphere ($L > 5.3$), whereas the fluxes given by Bell et al. represent an average of many satellite observations in the region $2.3 < L < 4$ which is most appropriate for MR whistler propagation. As a result of Landau damping, the wave power along the ray path varies as $P = P_0 \exp(-2\int k_i dS)$, where P_0 is the power at the injection point, k_i is the component of the imaginary part of the wave vector k directed along the ray path, and dS is an element of distance along the ray path. The quantity k_i is computed at each time step for each ray using the formulation given by *Brinca* [1972, equation 2]. Subsequent integration of k_i with respect to the distance traversed by the ray leads to the variation of the wave power density along the ray path. The real part of the refractive index μ (which is used to evaluate k_i) is calculated by the VLF ray tracing code [*Inan and Bell*, 1977] using the cold plasma approximation, which tends to overestimate μ very close to the resonance cone (where it would otherwise be bounded by thermal effects). This cold-plasma assumption leads to increased damping, and hence the lifetime values listed below should be treated as a lower bound to actual lifetimes, evaluated with the full thermal effects taken into account.

[8] To examine the effects of Landau damping, we launch rays from four assumed lightning source locations ($\lambda_s = 25°$,

35°, 45°, and 55°) at an altitude of 1000 km, with vertical wave normal angles, and from each location we trace rays in the frequency range 0.2–10 kHz in a smooth magnetosphere modeled after *Carpenter and Anderson* [1992] under geomagnetically quiet conditions ($K_p \approx 0$, resulting in plasmapause located at $L \approx 5.5$). We then compute the Landau damping along the path of each ray, note the time at which its power density is reduced by a total of 10 dB relative to its initial power density, and designate this value the lifetime $\tau(f, \lambda)$ of this particular ray. For example the lifetimes of the 0.5 kHz and 5 kHz rays launched at $\lambda = 25°$ are ~37 s and ~6 s, respectively, as can be inferred from Figures 1c and 1g. It should be noted that in calculating lifetimes, only wave power deposition due to Landau damping from the magnetosphere is considered. Geometrical effects such as spreading or focusing losses (or gains) are neglected in this preliminary treatment, as is the collisional power loss in the ionosphere.

[9] Lifetimes calculated as described above are shown in Figure 2. Waves at lower frequencies (≤1 kHz) have dramatically longer lifetimes than those at the higher frequencies, with the 200 Hz component launched at 25° lasting over 70 s. We note that wave frequency components below ~400 Hz are plotted as dashed lines to indicate that in order to propagate up to the radiation belts, they would have to undergo mode conversion from the left-hand polarized ion cyclotron mode into the right-hand polarized whistler mode in the ionosphere. Such mode coupling has been both experimentally observed [*Rodriguez and Gurnett*, 1971] and theoretically explained in previous work [*Arantes and Scarabucci*, 1975]. Nevertheless, when considering absolute power levels of such low-frequency wave components it is necessary to account for the power loss due to imperfect mode coupling. The lifetimes of MR whistlers decrease as the injection latitude of the rays is increased, regardless of the wave frequency. For injection latitudes lying in the range 25° to 45°, the lifetime of MR whistlers can be approximately expressed analytically as a function of wave frequency f (in kHz), and injection latitude λ (in degrees) as:

$$\tau(f,\lambda) = \frac{9 + 2^{6.1-\lambda/10}}{f^{0.925-0.005\lambda}}. \quad (2)$$

To understand the frequency and injection latitude dependence of MR whistler lifetimes, we refer to Figure 3a, which shows the equatorial LHR frequency (which is the also the frequency of waves which eventually settle at this L-shell) as a function of L-shell. In order to settle at the appropriate L-shell, a wave component at a given frequency propagates predominantly to either higher or lower L-shells relative to the L-shell of injection. In propagating from lower to higher L-shells, the wave frequency remains almost entirely below the LHR frequency, with the result that the wave refractive index (μ) surface is closed, the magnitude of μ is therefore bounded, and stays at relatively low values as shown in Figure 1d. If on the other hand, the ray path moves from higher to lower L-shells, the wave frequency remains above the LHR frequency, with a corresponding refractive index surface that is open, with consequent values of μ being unbounded and potentially very large. To move to lower L-shells, the $\boldsymbol{k}$-vector of the ray extends beyond the Gendrin angle [*Edgar*, 1972] and remains very close to the resonance cone, resulting in large values of μ. The large values of μ in turn imply lower phase (and group) velocities, which cause the waves to resonate with lower energy particles, of which there are many more (a condition necessary for Landau damping) than higher energy particles, thus resulting in significant damping.

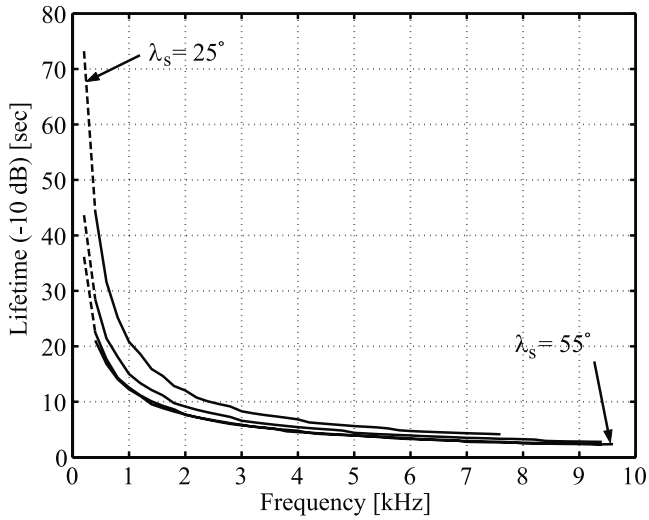

Figure 2. MR whistler lifetime (defined as the time when the wave power density along the ray path is diminished by 10 dB) plotted as a function of wave frequency for MR whistler wave, parameterized in injection latitude (showing λ_s = 25°, 35°, 45°, and 55°).

[10] For rays injected from ≥45° latitude and for the 200 Hz–10 kHz frequency range considered here, ray paths for all of the frequency components need to move from higher to lower L-shells, resulting in overall high μ values, increased damping rates, and decreased lifetimes. Note from Figure 2 that the lifetimes for 45° and 55° source latitude are very similar. For the lower injection latitude of 35°, some of the frequency components need to move to higher L-shells to reach their settling L-shells, and since these are primarily the low frequency components, their lifetimes are dramatically longer, whereas the lifetimes of the higher frequency components (≥5 kHz) differ only slightly from the ≥45° injection cases. For the lowest injection latitude considered of 25°, rays for most of the frequencies considered move from lower to higher L-shells, resulting in significantly larger lifetimes. An additional effect, which accounts for the slight differences between the 45° and 55° cases, is that rays launched from higher latitudes damp faster since they initially follow longer geomagnetic field lines.

4. Frequency Spectrum of Lightning-Generated Whistler Waves

[11] To determine the power spectral density of a typical vertical cloud-to-ground lightning discharge, we start with the radiation field component of the electric field at a distance D given [*Uman*, 1984, p. 61] as:

$$E = \frac{1}{4\pi\varepsilon_0 c^2 D}\left[\frac{d^2M}{dt^2}\right] = \frac{1}{4\pi\varepsilon_0 c^2 D} 2h_e \left[\frac{dI}{dt}\right], \quad (3)$$

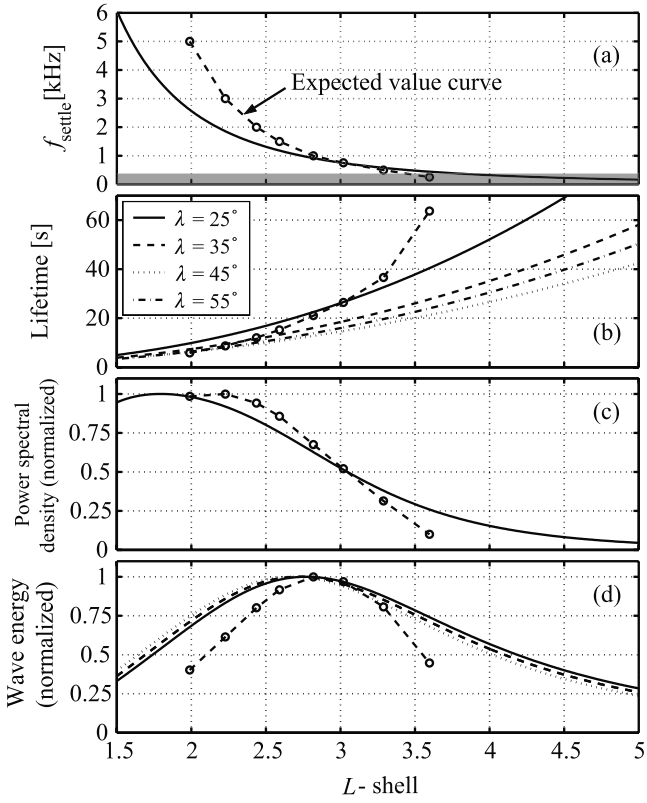

Figure 3. Determination of MR whistler energy deposition as a function of *L*-shell (a) settling frequency versus *L*-shell, the gray shaded region indicating frequency components which can only enter the magnetosphere upon mode conversion in the ionosphere (b) f_{settle} is replaced by its −10 dB lifetime, showing injection latitudes of 25° (solid line), 35° (dashed line), 45° (dotted line), and 55° (dash-dot line) versus *L*-shell, (c) f_{settle} is replaced by each frequency's lightning power spectral density plotted as function of *L*-shell normalized to its maximum value S(3.56 kHz) = 24 pW/m^2 at 100 km, and (d) the curves of Figures 2b and 2c are multiplied and the resulting curve is normalized to obtain an estimate of the distribution of energy deposited into the magnetosphere by lightning generated MR whistlers, as a function of *L*-shell. Dash-circle curve shows a similar analysis for expected-*L* values (see Figure 5).

where c is the velocity of light, ε_0 is the permittivity of free space, $M = 2h_eQ$ is the lightning dipole moment due to a total charge Q at a height of h_e above ground, $I = dQ/dt$ is the return stroke current, and the quantities in brackets are their retarded values obtained at time $(t - D/c)$. We model the return stroke current at VLF frequencies as a double exponential:

$$I(t) = I_0\left(e^{-bt} - e^{-at}\right), \tag{4}$$

giving radiated far-field, time domain electric field E, and associated power spectral density $S(\omega)$ in W/m^2/Hz as:

$$E(D) = \frac{1}{4\pi\varepsilon_0 c^2 D}(2h_eI_0)\left[ae^{-at} - be^{-bt}\right] \tag{5}$$

$$S(\omega) = \frac{1}{Z_0}\left(\frac{h_eI_0}{2\pi\varepsilon_0 c^2 D}\right)^2 \frac{\omega^2(a-b)^2}{(\omega^2 + a^2)(\omega^2 + b^2)}, \tag{6}$$

where $Z_0 = 377\ \Omega$ is the intrinsic impedance of free space, h_e is set to a typical assumed lightning stroke height of 5 km, and the model parameters a, b and I_0 are set to 5×10^3 sec^{-1}, 1×10^5 sec^{-1}, and −0.53 kA to give a typical spectrum which is broadly peaked between $f = 2$ kHz and $f = 6$ kHz, and gives E(100 km) = 10 V/m [*Lauben*, 1998].

5. *L*-Shell Distribution of MR Whistler Wave Energy

5.1. Analysis of Wave Energy Distribution Assuming $f_{settle} = f_{LHR}$

[12] From Figure 3a, we note that a wider range of frequency components settle at the lower *L*-shells, for instance, the region $3 \le L \le 5$ is occupied essentially by frequencies of $f \le 0.8$ kHz or a bandwidth of approximately 0.6 kHz, (i.e., spectral density of 0.3 kHz/*L*-shell), while the region $2 \le L \le 3$ is occupied by a bandwidth of 1.7 kHz (i.e., 1.7 kHz/*L*-shell), and $1.5 \le L \le 2$ by a bandwidth of ∼3.5 kHz (i.e., 7 kHz/*L*-shell). Based on the frequency spectrum of lightning, the most intense components are $3 \le f \le 6$ kHz, which tend to settle at the lowest *L*-shells. However, from Figure 2 we note that the low-frequency components are the more persistent, with dramatically longer lifetimes than their higher-frequency counterparts. The competing effects of intense, spectrally dense but short-lived high frequency components at low *L*-shells and weaker, spectrally diffuse but much longer-lived low frequency components at high *L*-shells suggest that there could be an *L*-region where the MR whistler wave energy is maximized.

[13] We examine this possibility in Figures 3b, 3c, and 3d. As mentioned before, Figure 3a is a plot of settling frequency versus *L*-shell, which is also a plot of the equatorial LHR frequency. We note once again that frequency components below ∼400 Hz must undergo mode conversion from the ion cyclotron mode to the whistler mode in the ionosphere in order to escape into the magnetosphere [*Rodriguez and Gurnett*, 1971; *Arantes and Scarabucci*, 1975]. These low-frequency components are included for completeness but shaded with gray to indicate that their power levels are likely to be lower due to imperfect coupling between right-hand (RH) and left-hand (LH) polarized modes. Figure 3b shows the lifetime at each *L*-shell of waves at the particular frequency that settles at that *L*-shell (as given in Figure 3a), calculated using (2) for $\lambda_s = 25°$, 35°, 45°, and 55°. For example, the $f = 2.5$ kHz component settles at $L = 2$ as shown in Figure 3a. The lifetime of the 2.5 kHz wave injected at $\lambda_s = 25°$ is ∼10 s as shown in Figure 3b, noting that the abscissa value shows the settling *L*-shell ($L = 2$) rather than the wave frequency ($f = 2.5$ kHz). The lifetimes shown in Figure 3b can be thought of as the lifetimes of MR whistlers on different *L*-shells, with the understanding that each *L*-shell is maximally illuminated (as discussed earlier in connection with Figures 3b and 3c and later in connection with Figure 5) by waves at a particular frequency (as given in Figure 3a). Figure 3c shows normalized wave power spectral density as a function of *L*-shell of waves at the particular frequency that settles at that *L*-shell (as given in Figure 3a), calculated using equation (6). Considering once again 2.5 kHz waves as a numerical example, the relative spectral power of the

2.5 kHz component is 0.98 relative to the maximum spectral component, as shown in Figure 3c, once again as a function of settling L-shell.

[14] This association between wave power spectral density and L-shell is valid only to the degree that each L-shell is illuminated maximally by waves at the particular frequency shown in Figure 3a, with the understanding that waves at a given frequency do also pass through (and deposit energy at) other L-shells as they migrate out to their settling L-shell, as discussed below in connection with Figure 5.

[15] The L-dependence of the MR whistler lifetime as shown in Figure 3b and the L-dependence of lightning-induced MR whistler wave power density as shown in Figure 3c can be simply multiplied to determine the L-dependence of MR whistler wave energy deposition. The resultant curve shown in Figure 3d indicates that there indeed is an L-shell region at which a maximum amount of MR whistler wave energy is deposited, as a result of the competing effects of increasing lifetimes and decreasing whistler wave power spectral density with increasing L-shell. The maximum in MR whistler energy deposition lies in the range $2.5 < L < 3$, a region known for reduced fluxes of energetic radiation belt particles, also referred to as the "slot region" [*Walt*, 1994, p. 80]. The concentration of MR whistler energy deposition in this region would necessarily lead to enhanced diffusion rates of energetic electrons into the loss-cone and may thus be responsible for the formation of the slot region between the inner and outer radiation belts. This idea fits well with previous work which shows that the slot region is formed as a natural balance between particles diffusing radially inward from higher L-shells and whistler-mode wave driven diffusion of particles into the loss cone at lower L-shells [*Lyons and Thorne*, 1973]. In most past work the source of whistler-mode waves was modeled to represent plasmaspheric hiss following *Lyons et al.* [1972], while in recent studies, the source of particle loss was expanded to include plasmaspheric hiss, coulomb collisions, anthropogenic VLF transmitters, and MR whistler waves [*Abel and Thorne*, 1998a, 1998b]. Based on the present work, showing the close association between extended lifetimes and the particular L-dependent wave energy distribution exhibited by MR whistlers, it is likely that MR whistler waves originating in lightning discharges play a more dominant role in the loss process than what was previously believed.

[16] To further illustrate the implications of the maximum in MR whistler wave energy and in terms of the formation of the slot region, we plot in Figure 4 the energy of counter-streaming electrons at the bounce loss-cone which undergo first order gyroresonance with MR whistler waves of different frequencies as a function of wave normal angle at the magnetic equator at $L = 2$ and $L = 3$. We see that energies of the electrons that would interact with MR whistler waves considered here extend from tens of keV to tens of MeV and even higher, which is the range of energies most depleted in the slot region. As the whistler waves approach their settling L-shell, the wave normal vector tends to the resonance cone, where higher order cyclotron resonance interactions begin to dominate. We note that although Figure 4 only shows resonant energies for equatorial first-order gyroresonance, the energies of electrons involved in off-equatorial and higher-order gyroresonance interactions are even higher and lie well within the range of electron energies for which the slot region is prominently observed [*Walt*, 1994; p. 80].

5.2. Inclusion of Path Losses in Determining f_{settle} and Resulting Energy Distribution

[17] Although the fact that the L-shell region of maximum MR whistler energy deposition is coincident with the slot region is suggestive of a causative association, the generality of this result needs to be assessed in terms of the degree to which the wave energy at a particular frequency is actually deposited at the settling L-shell. As noted previously in connection with Figure 1, MR whistlers take a finite amount of time to reach their settling L-shells so that not all of the wave energy at a given frequency is deposited at that particular L-shell. The foregoing discussion in connection with Figure 3 was based on the simplifying assumption that the MR whistler waves deposit all of their energy at the corresponding settling L-shell We now quantitatively consider the deposition of whistler wave energy everywhere along the ray path, and discuss the implications in terms of the generality of the result shown in Figure 3.

[18] We consider eight representative frequency components, namely 5, 3, 2, 1.5, 1, 0.75, 0.5, and 0.25 kHz, trace ray paths at each frequency component injected at 25° at 1000 km altitude and vertical wave normal angles, and calculate the damping until the wave power density reaches 1% of its initial value. The magnetosphere is divided into $0.1L$ wide "bins," and the power density of the wave at points sampled at 1 ms intervals along the ray path is added into the appropriate L-bin. Once the entire ray path has been sampled, the resultant total wave power-density is normalized and treated as the L-shell distribution of the wave energy at that particular frequency component. Resultant wave energy distributions for the 5 and 0.5 kHz frequency components are shown as an example in Figure 5.

[19] Using L-shell distributions for other frequencies (not shown) similar to those shown in Figure 5 for 0.5 and 5 kHz, we carry out a similar analysis as discussed earlier in connection with Figure 3 to determine the location in the magnetosphere where the maximum amount of MR whistler wave energy would be deposited. Instead of using the equatorial LHR frequency to associate each frequency component with a particular settling L-shell, we now calculate the expected value of the L-shell distribution for each frequency component and plot this value as the dash-circle curve in Figure 3a (the circles show the data points for 5, 3, 2, 1.5, 1, 0.75, 0.5, and 0.25 kHz), which represents the more realistic association between wave frequency and L-shell, which accounts for the deposition of wave energy at L-shells other than the settling L-shell. Figures 3b, 3c, and 3d, respectively show the lifetimes, normalized power density, and MR whistler energy deposition profiles corresponding to this more realistic case represented by the dash-circle curve in Figure 3a.

[20] Figure 3a shows that the actual (or expected) L-shell of deposition differs significantly from the so-called settling L-shell represented by the equatorial LHR frequency. In particular, the higher-frequency components initially propagate to higher L-shells before returning to their settling L-shells and in so doing are damped well before they

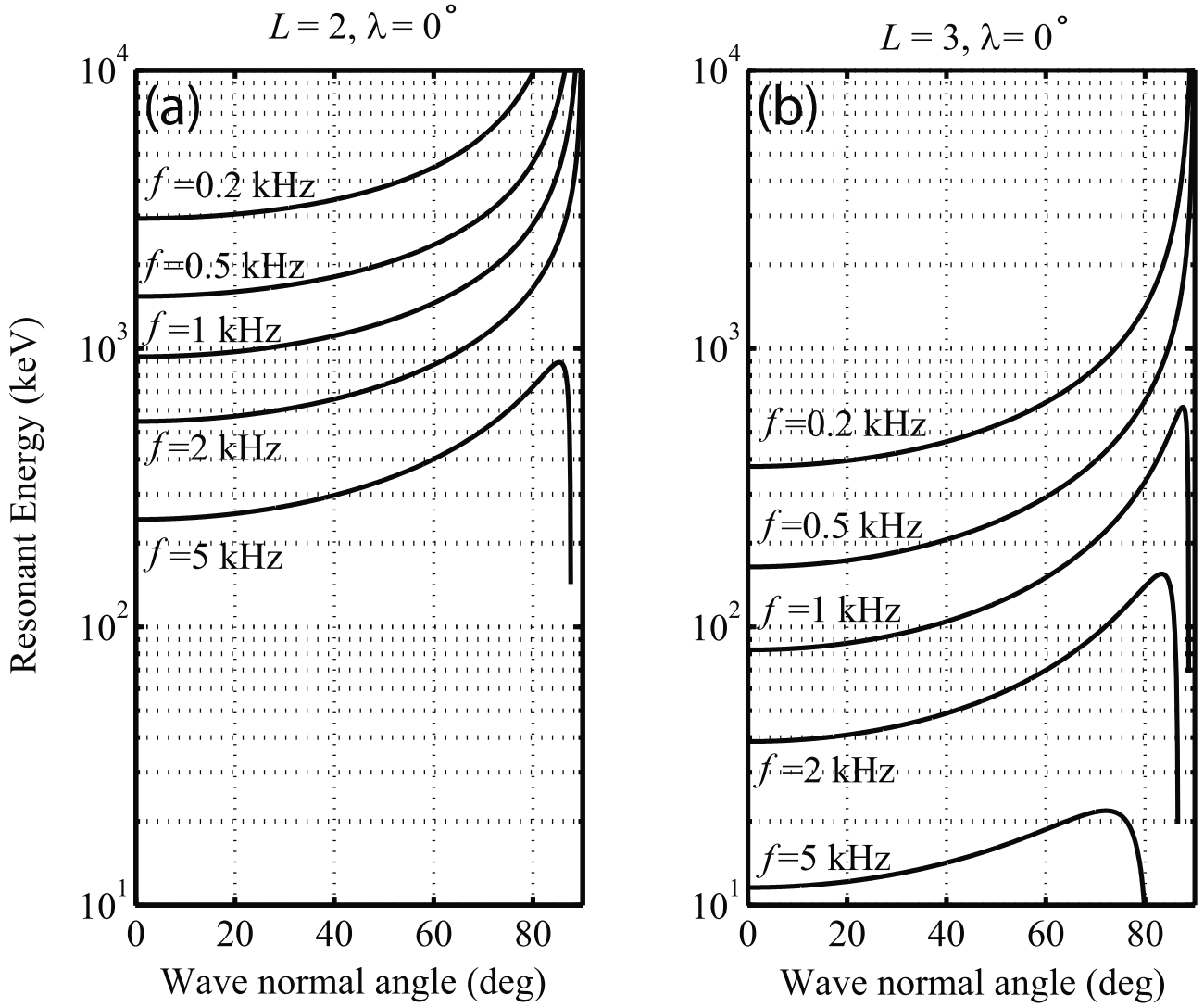

Figure 4. Energy of near-loss-cone counter-streaming electrons in first order gyroresonance with whistler waves of different frequencies, plotted as a function of wave normal angle at the magnetic equator at (a) $L = 2$ and (b) $L = 3$.

settle. The expected L-shell of deposition for such rays is higher than the settling L-value. The lower frequencies, on the other hand, spend a significant portion of their time propagating to their settling L-shell and so their expected-L location tends to be lower than the settling L-shell as determined by the corresponding equatorial LHR value. The net effect of using the expected-L value as opposed to settling L-shells can be seen most clearly in Figure 3d, where we observe that the peak in MR whistler wave energy deposition has become sharper. However, the location of the peak has basically remained near $L \approx 2.8$.

5.3. Discussion

[21] The fact that MR whistler wave energy peaks in the vicinity of the slot region suggests a tantalizing causal relationship that we now discuss in light of past work. In particular we note the work of *Abel and Thorne* [1998a, 1998b], who have calculated scattering rates and electron lifetimes due to plasmaspheric hiss, coulomb interactions, whistlers, and anthropogenic VLF transmitters and have concluded that in the vicinity of the slot region whistlers are indeed important drivers of scattering, with plasmaspheric hiss dominating at higher L-shells and VLF transmitters becoming more important towards the outer edge of the inner zone. We now use simple scaling of the results of the Abel and Thorne analysis to qualitatively show that MR whistlers could play a more dominant role in the formation and maintenance of the slot region than previously assumed.

[22] *Abel and Thorne* [1998a, 1998b] modeled MR whistlers as an incoherent band of frequencies at 4.5 kHz ± 2 kHz, extending between $L = 1.2$ and $L = 4$, with an average wave normal angle of 45° ± 22.5°. Other parameters were taken from ducted whistler statistics and shown to be approximately valid for MR whistlers, namely an intensity of 10 pT and duration of 30 ms (or intensity of 3 pT and duration of 0.3 s), with a rate of 60/min giving an occurrence rate of 3%. The analysis showed that for lower energy electrons (~100 keV), MR whistlers were most

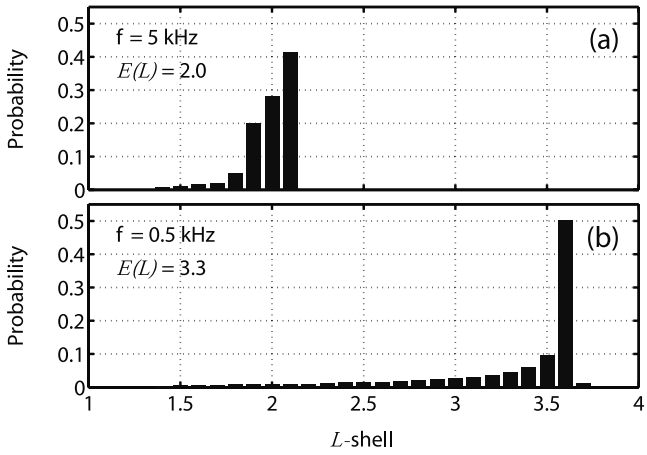

Figure 5. Distribution function of MR whistler wave energy as a function of L-shell in 0.1 L bins for the frequency components (a) 5 kHz, and (b) 0.5 kHz. The power of each ray is Landau damped, sampled along its trajectory at 1 ms intervals, and added into the appropriate bin.

effective at controlling the lifetime at $L \approx 3$, and that this region of MR whistler effectiveness moved closer to the Earth with increasing energy, such that for example for 1500 keV electrons, MR whistlers played a dominant role at $L \approx 2.2$.

[23] In light of the present and previous works we now discuss several refinements to the assumptions of *Abel and Thorne* [1998a, 1998b]. We begin by examining the general condition for wave/particle resonance given by equation (7) and field-aligned component of the wave vector $k_{\|}$ given by equation (8) below:

$$\omega - k_{\|}\nu_{\|} = -n\Omega_H/\gamma \tag{7}$$

$$k_{\|} = \omega\mu\ \cos(\theta)/c, \tag{8}$$

where ω is the wave frequency, $\nu_{\|}$ is the field-aligned component of the particle velocity, n is the resonance number, Ω_{H} is the electron gyrofrequency, γ is the relativistic Lorentz correction factor, μ is the refractive index, θ is the angle of the wave vector with respect to the static magnetic field, and c is the speed of light. Combining equations (7) and (8) we obtain equation (9):

$$\left(1 - \nu_{\|}\mu\cos(\theta)/c\right) = -n\Omega_H/\gamma\omega. \tag{9}$$

If, instead of assuming that the MR whistler waves occupy a constant frequency band throughout the plasmasphere, we assume that they occupy a band centered on the local LHR frequency as has been discussed above and by previous authors [*Thorne and Horne*, 1994; *Ristic'-Djurovic' et al.*, 1998], then both ω and the gyrofrequency vary approximately as L^{-3} in the inner plasmasphere. Such a variation would in turn imply that $\nu_{\|}$ and (hence particle resonant energy) would be approximately independent of L.

[24] In addition we have shown in the present work that the product of wave power and duration does not stay constant throughout the plasmasphere as was assumed by *Abel and Thorne* [1998a, 1998b] but rather that this product exhibits a maximum in the vicinity of the slot region. This assertion is partly confirmed (because Edgar only counted MR whistler components and did not examine their energy content) by *Edgar* [1976, p. 77] who has shown that although MR whistlers can occur at $1.2 < L < 4$ the distribution is not uniform, showing strong localization between $2 < L < 3$, with a maximum of $\approx$15.4 components/min occurring at $2.2 < L < 2.4$.

[25] Applying the two modifications discussed above to the analysis of *Abel and Thorne* [1998a], we expect all electron energies to be affected in roughly the same manner as a function of L-shell and scattering rates in the vicinity of the slot region to be approximately 2 times larger than those obtained using Abel and Thorne's original assumptions (with a corresponding scattering rate reduction at $3.5 < L < 2$).

[26] Based on the foregoing discussion and building upon previous work that has dealt with assessing scattering rates in the vicinity of the slot region [*Abel and Thorne*, 1998a, 1998b], we believe that MR waves could play a more dominant role in the formation and maintenance of the slot region than previously supposed. While this conclusion is a slight modification of the conclusions of past studies [*Abel and Thorne*, 1998a, 1998b], it fits well with the generally accepted mechanism of slot-region formation which is essentially a balance between particles diffusing radially inwards from higher L-shells, and particles scattered into the loss cone by resonant interactions with waves and other loss processes [*Lyons et al.*, 1971; *Lyons and Thorne*, 1973]. Previous assessments of the distribution of lightning generated whistler waves in the magnetosphere have only considered "ducted" waves [*Burgess and Inan*, 1993]. Similar efforts for nonducted whistlers have yielded mixed results [*Sonwalker and Inan*, 1989; *Draganov et al.*, 1992, 1993; *Thorne and Horne*, 1994] leading to contradicting conclusions. We believe that with the more recent and richer data sets obtained from the HYDRA instrument aboard the POLAR satellite [*Bell et al.*, 2002], a more accurate estimate can be made of the suprathermal particle fluxes that lead to Landau damping and hence of the overall distribution and spatial structure of MR whistler wave energy that populates the magnetosphere.

[27] We note also that not all MR whistler injection latitudes contribute uniformly to the formation of the slot region. Figure 2 shows that as the lightning injection latitude is increased, the lifetimes of MR whistlers become significantly shorter, meaning that lightning discharges at lower latitudes dominate in terms of deposition of whistler wave energy in the plasmasphere. In addition, lightning occurrence statistics indicate that low-latitude lightning discharges are significantly more numerous those at higher latitudes [*Orville and Spencer*, 1979] so that there is far more energy injected in the form of MR whistlers originating at low latitudes. The dominance of low-latitude MR whistlers does not extend all the way to the equator; we support the conclusion of *Thorne and Horne* [1994] that below $\sim$15° whistlers do not escape out of the ionosphere

and hence cannot magnetospherically reflect. In addition, as whistler waves propagate through the ionosphere, the transionospheric collisional damping rates increase dramatically near the equator [*Helliwell*, 1965]. Using lightning occurrence versus latitude data [*Orville and Spencer*, 1979] combined with the latitude dependant trans-ionospheric damping rates, we find that the region of maximum whistler escape energy peaks at approximately 25°–35° degrees geomagnetic latitude, which is the focus of attention in the present work.

[28] Our particular choice of vertical wave normal angles at the injection point of the rays deserves discussion: it is certainly true that initial wave normal angles need not be vertical at the topside ionosphere [*James*, 1972] and can in general be confined to a cone of $\sim 10^\circ$ about the vertical. This spreading of the initial wave normal angles can in turn influence the lifetime of the wave energy along the ray path [*Thorne and Horne*, 1994]. In this work we have chosen not to explicitly present the effects of nonvertical initial wave normal angle because while deviations from vertical do affect lifetimes, the general trend of the lifetime-versus-frequency remains roughly constant (much like the case shown in Figure 3b, where injection latitude changes absolute lifetime values, but not the general trend of the frequency dependence) so that upon normalizing, Figure 3d remains essentially unchanged.

6. Conclusions

[29] Different wave frequency components constituting a lightning-generated MR whistler wave packet tend to settle on a preferred *L*-shell in the magnetosphere, if allowed to propagate indefinitely. The lower frequency components settle at higher *L*-shells whereas the higher frequency components settle at lower *L*-shells. This preferred (or settling) *L*-shell is that at which the wave frequency is approximately equal to the equatorial lower hybrid resonance frequency.

[30] Associated with each frequency component of the MR whistler wave is a certain lifetime which we have computed using the Landau damping formulation of *Brinca* [1972] and representative plasmaspheric suprathermal particle fluxes obtained from the HYDRA instrument aboard the POLAR satellite [*Bell et al.*, 2002] and an initial power spectral density associated with the particular lightning discharge.

[31] The combination of the MR whistler lifetimes with the power spectral density of lightning radiation is used to determine the resultant MR whistler energy deposition as a function of *L*-shell in the magnetosphere. A prominent feature of this analysis is a clear maximum in energy deposition in the vicinity of the slot region. This result comes about due to the fact that low frequency components which settle at higher *L*-shells have a long lifetime but relatively low power spectral density, whereas higher frequency components which settle at low *L*-shells have a short lifetime but a relatively high power spectral density. The competition between lifetime and power spectral density results in the maximum in MR whistler wave energy at $L \approx 2.8$.

[32] We further note that the energies of electrons that undergo cyclotron resonance interactions with the whistler wave frequencies considered here, lie in the tens of keV to tens of MeV range (even higher for off-equatorial and higher gyroresonance interactions). Based on the preliminary analysis presented above, we conclude that the preferential accumulation of MR whistler wave energy in the vicinity of the slot region would lead to enhanced diffusion rates of energetic particles and could potentially result in the formation of the slot region.

[33] **Acknowledgments.** This research was supported by the Air Force Office of Scientific Research under grant F49620-99-1-0339-P00001, as well as by NASA grant NAS5-30371 via subcontract from the University of Iowa.

[34] Arthur Richmond thanks Vikas Sonwalker and another reviewer for their assistance in evaluating this paper.

References

Abel, B., and R. M. Thorne, Electron scattering loss in Earth's inner magnetosphere: 1. Dominant physical processes, *J. Geophys. Res.*, *103*(A2), 2385–2396, 1998a.

Abel, B., and R. M. Thorne, Electron scattering loss in Earth's inner magnetosphere: 2, Sensitivity to model parameters, *J. Geophys. Res.*, *103*(A2), 2397–2407, 1998b.

Arantes, D. S., and R. R. Scarabucci, Full-wave analysis and coupling effects in a crossover region, *Radio Sci.*, *10*(8–9), 801–811, 1975.

Bell, T. F., U. S. Inan, and J. Bortnik, The Landau damping of magnetospherically reflected whistlers within the plasmasphere, *Geophys. Res. Lett.*, *29*(15), 1733, doi:10.1029/2002GL014752, 2002.

Bortnik, J., U. S. Inan, and T. F. Bell, *L*-dependence of energetic electron precipitation driven by magnetospherically reflecting whistler waves, *J. Geophys. Res.*, *107*(A8), 1150, doi:10.1029/2001JA000303, 2002.

Brinca, A. L., On the stability of obliquely propagating whistlers, *J. Geophys. Res.*, *77*(19), 3495–3507, 1972.

Burgess, W. C., and U. S. Inan, The role of ducted whistlers in the precipitation loss and equilibrium flux of radiation belt electrons, *J. Geophys. Res.*, *98*(A9), 15,643–15,665, 1993.

Carpenter, D. L., and R. R. Anderson, An ISEE/whistler model of equatorial electron density in the magnetosphere, *J. Geophys. Res.*, *97*(A2), 1097–1108, 1992.

Draganov, A. B., U. S. Inan, V. S. Sonwalker, and T. F. Bell, Magnetospherically reflected whistlers as a source of plasmaspheric hiss, *Geophys. Res. Lett.*, *19*, 233, 1992.

Draganov, A. B., U. S. Inan, V. S. Sonwalker, and T. F. Bell, Whistlers and plasmaspheric hiss: Wave directions and three-dimensional propagation, *J. Geophys. Res.*, *98*(A7), 11,401–11,410, 1993.

Edgar, B. C., The structure of the magnetosphere as deduced from magnetospherically reflected whistlers, Ph.D. thesis, Radio Sci. Lab., Stanford Electron. Lab., Stanford Univ., Palo Alto, Calif., 1972.

Helliwell, R. A., *Whistlers and Related Ionospheric Phenomena*, Stanford Univ. Press, Palo Alto, Calif., 1965.

Inan, U. S., and T. F. Bell, The plasmapause as a VLF waveguide, *J. Geophys. Res.*, *82*(19), 2819–2827, 1977.

Kimura, I., Effects of ions on whistler-mode ray tracing, *Radio Sci.*, *1*, 269, 1966.

Lauben, D., Precipitation of radiation belt electrons by obliquely propagating lightning-generated whistler waves, Ph.D. thesis, Telecomm., Radio Sci. Lab., Stanford Univ., Palo Alto, Calif., 1998.

Lundin, B., and C. Krafft, On the similarity features of normalized frequency spectrograms of magnetospherically reflected whistlers, *J. Geophys. Res.*, *106*(A11), 25,643–25,654, 2001.

Lyons, L. R., and R. M. Thorne, Equilibrium structure of radiation belt electrons, *J. Geophys. Res.*, *78*(13), 2142–2149, 1973.

Lyons, L. R., R. M. Thorne, and C. F. Kennel, Electron pitch-angle diffusion driven by oblique whistler-mode turbulence, *J. Plasma Phys.*, *6*(3), 589–606, 1971.

Lyons, L. R., R. M. Thorne, and C. F. Kennel, Pitch-angle diffusion of radiation belt electrons within the plasmasphere, *J. Geophys. Res.*, *77*(19), 3455–3474, 1972.

Orville, R. E., and D. W. Spencer, Global lightning flash frequency, *Mon. Weather Rev.*, *107*, 934–943, 1979.

Ristic'-Djurovic', J. L., T. F. Bell, and U. S. Inan, Precipitation of radiation belt electrons by magnetospherically reflecting whistlers, *J. Geophys. Res.*, *103*(A5), 9249–9260, 1998.

Rodriguez, P., and D. A. Gurnett, An experimental study of very low-frequency mode coupling and polarization reversal, *J. Geophys. Res.*, *76*(4), 960, 1971.

Smith, R. L., and J. J. Angerami, Magnetospheric properties deduced from OGO 1 observations of ducted and nonducted whistlers, *J. Geophys. Res.*, *73*, 1, 1968.

Sonwalker, V. S., and U. S. Inan, Lightning as an embryonic source of VLF hiss, *J. Geophys. Res.*, *94*(A6), 6986–6994, 1989.

Thorne, R. M., and R. B. Horne, Landau damping of magnetospherically reflected whistlers, *J. Geophys. Res.*, *99*(A9), 17,249–17,258, 1994.

Uman, M. A., *Lightning*, Dover, Mineola, N.Y., 1984.

Walt, M., *Introduction to Geomagnetically Trapped Radiation*, *Atmos. and Space Sci. Ser.*, Cambridge Univ. Press, New York, 1994.

T. F. Bell, J. Bortnik, and U. S. Inan, Space, Telecommunications, and Radio Science Group, Stanford University, Room 306 David Packard Building, 350 Serra Mall, Stanford, CA 94305-7396, USA. (bell@nova.stanford.edu; jbortnik@stanford.edu; inan@nova.stanford.edu)